Microwave spectrum of the MnO radical in the X 6 Σ + state

Kei-ichi Namiki and Shuji Saito

Citation: The Journal of Chemical Physics **107**, 8848 (1997); doi: 10.1063/1.475176
View online: http://dx.doi.org/10.1063/1.475176
View Table of Contents: http://scitation.aip.org/content/aip/journal/jcp/107/21?ver=pdfcov
Published by the AIP Publishing

Microwave spectrum of the MnO radical in the $X\ ^6\Sigma^+$ state

Kei-ichi Namiki and Shuji Saito
The Graduate University for Advanced Studies and the Institute for Molecular Science, Myodaiji, Okazaki 444, Japan

(Received 6 June 1997; accepted 29 August 1997)

The microwave spectrum of MnO in the $^6\Sigma^+$ ground electronic state was detected using a source-modulated submillimeter-wave spectrometer. The MnO radical was efficiently generated by dc sputtering of manganese flakes placed inside a hollow cathode in the presence of an oxygen and helium mixture. In total, 283 spectral lines were measured in the frequency region of 210–450 GHz for nine rotational transitions, each of which showed six fine structure line groups consisting of several hyperfine structure components due to the ^{55}Mn nucleus ($I=5/2$). A least-squares analysis of the measured line frequencies resulted in the determination of rotational, fine, and hyperfine coupling constants including higher-order spin–orbit distortion terms for the spin–spin, spin–rotation interactions and the Fermi contact interaction of the Mn nucleus. The hyperfine coupling constants were used to assess plausible molecular orbital bonding models. © *1997 American Institute of Physics.* [S0021-9606(97)03145-0]

INTRODUCTION

Characterizing the ground and low-lying states of the $3d$ transition metal containing diatomic free radicals is challenging because of the high density of states with nonzero projection of the orbital and spin angular momentum. The most insightful information comes from the interpretation of the magnetic hyperfine parameters, which to a good approximation are simple expectation values of the geometric coordinates and the spin density of the valence electrons. Extensive spectroscopic studies of the magnetic hyperfine interactions have been made on the $3d$ metal monoxides from ScO to CuO. These studies have revealed that the bonding in the $3d$ transition metal oxides is surprisingly complex, consisting of both an ionic and covalent component.[1,2] A single configuration description appears qualitatively accurate for the early transition metal oxides. In these cases the metal $3d$ and $4s$ orbitals simultaneously form molecular orbitals with the $2p$ orbitals of the oxygen atom. Specifically, the metal orbitals undergo $sd\sigma$ hybridization, and there is a bonding and antibonding molecular orbital formation between the hybrid polarized toward the O atom and the O $2p\sigma$ orbital. The hybrid orbital polarized away from the O atom is nonbonding. The $3d\pi$ and $2p\pi$ orbitals also form bonding and antibonding orbitals to facilitate backdonation of the doubly occupied O $2p\pi$ into empty metal $3d\pi$ orbitals. The $3d\delta$ orbitals are nonbonding. The energy order of the molecular orbitals is σ bonding$<\pi$ bonding$<\sigma$ nonbonding$\approx\delta$ nonbonding $<\pi$ antibonding$<\sigma$ antibonding.[2] There is a delicate balance between the lost energy in $3d-3d$ exchange, stabilization gained by backdonation, and the energy associated with hybridization that dictates the filling order of the molecular orbitals. Upon filling the σ and π bonding molecular orbitals minimizing the $3d-3d$ exchange energy lost appears to dominate.

Among the $3d$ metal oxides MnO has the ground electronic state of $^6\Sigma^+$ with the highest spin multiplicity and a single manganese isotopic species of $I=5/2$. The optical spectrum of MnO was first reported by Gupta in 1934,[3] but not characterized until 1975 by Pinchemel and Schamps.[4] They assigned and analyzed the rotational and fine structures of the (1,0) band of $A\ ^6\Sigma^+-X\ ^6\Sigma^+$. Although the spectrum observed was a parallel-type transition of $\Delta\Lambda=0$, they determined the spin–spin coupling constant for both excited and ground electronic states, $\lambda'=0.00\pm0.05\ \mathrm{cm}^{-1}$ and $\lambda''=0.66\pm0.05\ \mathrm{cm}^{-1}$, respectively, based on the relative positions of six subband heads. Weltner and his collaborators[5,6] studied the ESR spectrum of several manganese oxides in various inert gas matrices at 4 K. They determined the ^{55}Mn($I=5/2$) isotropic and dipolar hyperfine coupling constants of MnO on the assumption of a positive sign for $A_\parallel$ and $A_\perp$, giving $A_{\mathrm{iso}}=353$ MHz and $A_{\mathrm{dip}}=-86$ MHz and discussed contributions of the Mn atomic orbital components to the hyperfine coupling constants. More recently, Gordon and Merer[7] studied the (0,0), (0,1), and (1,0) bands of the $A\ ^6\Sigma^+-X\ ^6\Sigma^+$ electronic transition of MnO with a high dispersion photograph, and reported that the electronic transition was an exceptionally complicated spectrum because of the high spin multiplicity, the manganese hyperfine structure, and the numerous rotational perturbations in the excited electronic state. They found a new type of perturbation due to a mixing of spin components through hyperfine matrix elements, and the observed extra lines due to this mixing made it possible to determine the fine structure parameters for the two electronic states. Recently Adam *et al.*[8] studied the same electronic transition at sub-Doppler resolution using intermodulated fluorescence spectroscopy. They found an anomalous structure, which was explained by internal hyperfine perturbations in both electronic states and reported revised molecular constants for the $X\ ^6\Sigma^+\ v=0$ state and the $A\ ^6\Sigma^+$ $v=1$ state.

The MnO radical has been subjected to numerous *ab initio* calculations.[2,9–11] Pinchemel and Schamps[9] carried out SCF calculations on MnO with single- and double-zeta STO basis sets and reported SCF energies for several excited electronic states, SCF wave functions, and population analysis.

 0021-9606/97/107(21)/8848/6/$10.00

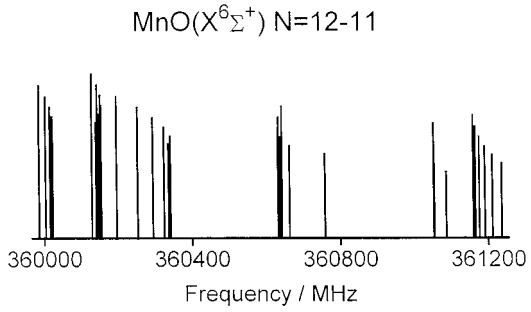

FIG. 1. Stick diagram of observed spectral lines of the $N=12-11$ transition of MnO($^6\Sigma^+$) in the 360 GHz region.

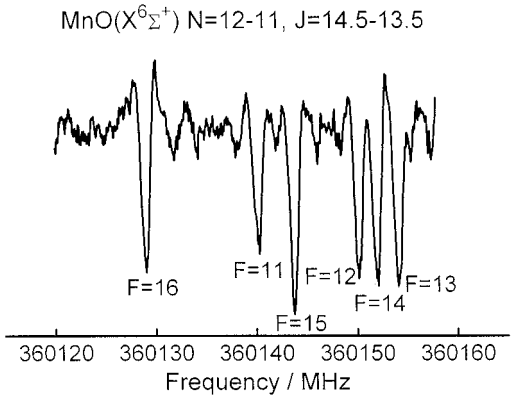

FIG. 2. An example of the observed spectral lines of MnO($^6\Sigma^+$): the F_1 component of the $N=12-11$ transition. The lower-level quantum number of the hyperfine structure due to the manganese nucleus $I=5/2$ is shown below the peak of each component. A hundred scans were integrated with a rate of about six scans per second. The PSD time constant was 1 ms.

Bauschlicher and Maitre[2] calculated the equilibrium bond length, the dissociation energy, the equilibrium vibrational frequency, and the dipole moment for the first-row transition metal oxides and sulfides with several high-level *ab initio* methods such as a coupled cluster singles and doubles (CCSD) technique. Recently, Bakalbassis *et al.*[11] studied ground and low-lying excited state properties of the first-low transition metal oxides by using an improved atom superposition and electron delocalization molecular orbital (ASED-MO) method.

In the present study we measured the pure rotational transitions of MnO in the submillimeter-wave region, and determined its molecular constants, including detailed hyperfine coupling constants and also higher-order spin–orbit distortion terms.

EXPERIMENT

Spectral lines of MnO were observed by using a 100 kHz source modulated submillimeter-wave spectrometer in conjunction with a 2 m long free-space absorption cell.[12,13] The MnO radical was generated in the gas mixture of oxygen and helium by dc sputtering of manganese flakes placed inside the cylindrical stainless-steel hollow cathode. The spectral lines of MnO predicted from the known molecular constants[8] were searched for in the 360 GHz region at a discharge current of several hundred mA with the cell maintained below $-170\,^\circ$C. Many spectral lines appeared in the predicted frequency region and they exhibited a large Zeeman effect at a magnetic field of about 30 Gauss, which were appropriate for transitions in the $^6\Sigma^+$ electronic state.[14] The spectral lines were composed of six separate groups, each of which had as many as six lines, as shown in Fig. 1. A similar spectral pattern, including nearly the same number of lines, was observed in the 330 GHz frequency region. Hence, the spectral lines detected in each frequency region were assigned to be components of a rotational transition of the MnO radical in the $X\ ^6\Sigma^+$ state: six fine structure line groups, each of which consists of six manganese hyperfine structure components.

The spectral lines increased in intensity with the discharge current up to 500 mA, but under high-current discharge conditions the spectral intensity gradually decreased after a few minutes. This was considered to be mainly due to a rise in the temperature of the cell and the hollow cathode inner surface. The spectral intensity recovered after about a ten minute interruption of the discharge. Therefore, the discharge current was maintained at 300 mA. The optimum condition for the production of MnO was obtained at the partial pressures of 5 mTorr of oxygen and 5–8 mTorr of helium. The typical signal to noise ratio of a spectral line observed is shown in Fig. 2. Each line frequency was determined by averaging five pairs of upward and downward frequency sweep measurements. The frequency measurement error ranges from 10 to 20 kHz. In total, 283 lines were measured in the frequency region of 210–450 GHz, as listed in Table I.

ANALYSIS

The following Hamiltonian was used in the analysis of the observed spectral lines of MnO in the $X\ ^6\Sigma^+$ electronic state:[7]

$$H=H_{\rm rot}+H_{\rm ss}+H_{\rm sr}+H_{\rm hfs},$$

where $H_{\rm rot}$ denotes the rotational Hamiltonian including the centrifugal distortion effect, $H_{\rm ss}$ the spin–spin interaction term with its centrifugal distortion effect, $H_{\rm sr}$ the spin–rotation interaction including its centrifugal distortion effect, and $H_{\rm hfs}$ the hyperfine interaction terms.[15] Furthermore, it immediately became evident that higher-order spin–orbit distortion terms were necessary to explain the observed line frequencies. The higher-order spin–orbit distortion terms are given as follows:

$$H_{\rm SO}^{(4)}=\Theta[35S_z^2-30\mathbf{S}^2S_z^2+25S_z^2-6\mathbf{S}^2+3\mathbf{S}^4]/12,$$

for the fourth order spin–orbit distortion coupling term,[16,17]

$$H_{\rm sr}^{(3)}=CT^3(\mathbf{L}^2,\mathbf{N})T^3(\mathbf{S},\mathbf{S},\mathbf{S})$$

and

$$\gamma_s=C\langle\Lambda|T_{q=0}^2(\mathbf{L}^2)|\Lambda\rangle/(10/\sqrt{6}),$$

TABLE I. Observed rotational transitions of MnO ($X\ ^6\Sigma^+$) (MHz).[a]

J[b]	$\nu_{J-5/2}$[c]	$\nu_{J-3/2}$[c]	$\nu_{J-1/2}$[c]	$\nu_{J+1/2}$[c]	$\nu_{J+3/2}$[c]	$\nu_{J+5/2}$[c]
$N=6$[b]						
3.5					212 374.726(−4)	212 437.455(12)
4.5					212 809.786(45)	212 757.604(−29)
5.5					210 937.271(6)	210 895.700(−25)
6.5				209 769.167(37)	209 690.645(22)	209 587.239(−13)
7.5	209 341.566(4)	209 354.180(51)	209 353.581(19)	209 339.222(29)	209 310.169(16)	209 265.445(18)
8.5	209 795.199(17)	209 819.736(68)[d]	209 829.778(16)	209 825.331(24)	209 806.108(8)	209 771.899(13)
$N=7$						
4.5				241 741.130(−43)	241 754.486(12)	241 799.597(11)
5.5		242 241.033(−39)	242 189.556(−42)	242 145.352(−36)	242 108.512(−11)	242 078.920(−6)
6.5	241 023.395(−14)	240 930.564(32)	240 872.017(−29)	240 832.679(−6)	240 804.822(13)	240 785.268(−23)
7.5	239 988.405(−1)	240 008.092(40)	239 991.085(−6)		239 881.171(12)	239 795.189(−12)
8.5	239 559.532(−25)	239 568.859(18)	239 567.802(−31)	239 555.953(−7)	239 532.484(−1)	239 496.550(−1)
9.5	239 897.418(19)	239 917.167(−11)	239 925.275(18)	239 921.501(5)	239 905.690(−28)	239 877.721(16)
$N=8$						
5.5			271 430.554(−22)	271 416.350(−18)	271 426.840(−2)	271 460.960(25)
6.5	271 847.042(−13)	271 801.083(−23)	271 762.189(−31)	271 730.375(−6)	271 705.446(−8)	271 687.208(17)
7.5	270 912.076(−1)	270 819.872(14)	270 772.211(21)	270 745.158(48)	270 729.596(−11)	270 722.734(−6)
8.5	270 114.679(26)	270 130.505(5)	270 113.519(5)	270 074.134(−55)	270 017.209(−4)	269 942.859(12)
9.5	269 722.532(−3)	269 729.655(46)	269 728.384(−23)	269 718.426(−12)	269 699.074(−7)	269 669.615(0)
10.5	269 979.536(35)	269 995.813(10)	270 002.432(23)	269 999.210(16)	269 986.002(−1)	269 962.663(15)
$N=9$						
6.5	301 318.545(41)	301 268.267(28)	301 238.478(371)[d]	301 227.642(47)	301 235.759(−297)[d]	301 262.824(97)[d]
7.5	301 562.495(28)	301 525.579(−1)	301 495.231(29)	301 471.251(44)	301 453.384(6)	301 441.429(13)
8.5	300 841.555(0)	300 748.976(15)	300 710.190(13)	300 691.808(0)		
9.5	300 209.369(9)	300 221.618(18)	300 204.458(−18)	300 168.764(−1)	300 118.279(−27)	300 052.005(23)
10.5	299 847.471(−31)	299 853.008(−21)	299 851.735(−27)	299 843.247(−30)	299 827.024(−23)	299 802.454(−8)
11.5	300 045.819(2)		300 064.932(−45)	300 062.170(−27)	300 050.987(−16)	300 031.228(−6)
$N=10$						
7.5	331 180.351(−1)	331 140.821(−18)	331 117.336(79)[d]	331 109.218(16)	331 116.152(−24)	331 137.631(23)
8.5	331 371.606(−4)	331 341.421(8)	331 317.048(2)	331 298.329(−3)	331 285.030(1)	331 276.833(−6)
9.5	330 793.765(−30)	330 700.080(32)	330 668.879(−25)	330 656.958(−22)	330 654.852(5)	330 660.743(3)
10.5	330 281.820(−11)	330 290.451(−48)	330 273.213(29)	330 240.323(−5)	330 194.858(14)	330 134.238(−25)
11.5	329 944.452(−30)	329 948.890(−4)	329 947.579(−50)	329 940.297(−23)	329 926.502(−15)	329 905.654(−46)
12.5	330 098.982(15)	330 110.536(−42)	330 115.187(−32)	330 112.788(−3)	330 103.134(−37)	330 086.194(−25)
$N=11$[c]						
8.5	361 086.380(−81)[d]	361 054.640(30)				361 052.758(−19)
9.5	361 236.074(52)	361 210.922(39)	361 190.927(13)	361 175.874(−48)	361 165.666(−1)	361 159.844(−19)
10.5	360 758.423(−104)[d]	360 663.083(−28)	360 638.736(11)	360 631.670(−33)	360 633.325(23)	360 642.514(9)
11.5	360 337.154(−23)	360 342.293(6)	360 324.780(−2)	360 294.278(18)	360 252.699(−2)	360 196.290(−7)
12.5	360 019.594(−30)	360 023.252(42)	360 021.988(6)	360 015.603(−17)	360 003.731(−6)	359 985.857(−28)
13.5	360 140.553(18)	360 150.494(−27)	360 154.489(1)	360 152.364(18)	360 143.972(−15)	360 129.278(−10)
$N=12$						
9.5	391 017.656(−29)	390 991.536(52)	390 975.890(2)[e]	390 970.869(20)	390 975.890(2)[e]	390 990.528(−13)
10.5	391 133.928(−5)	391 112.682(−16)	391 096.043(1)	391 083.764(−8)	391 075.678(21)	391 071.394(−41)
11.5		390 632.081(20)	390 613.647(−85)[d]	390 610.552(46)	390 614.757(15)	390 626.194(17)
12.5	390 378.274(−5)	390 379.966(71)[d]	390 362.252(12)	390 333.714(29)	390 295.322(13)	390 242.039(64)[d]
13.5	390 076.711(−87)[d]	390 079.810(52)	390 078.514(−70)[d]	390 072.980(−16)	390 062.676(19)	390 047.208(29)
14.5	390 171.453(−4)	390 180.082(−51)	390 183.609(50)	390 181.715(61)[d]	390 174.324(3)	390 161.444(−6)
$N=13$						
10.5	420 962.721(−104)[d]	420 940.680(−18)[e]	420 928.011(−7)[e]	420 923.801(31)	420 928.011(−7)[e]	420 940.680(−18)[e]
11.5	421 052.116(−13)	421 033.940(−26)	421 019.829(−38)	421 009.646(0)	421 003.084(−3)	420 999.944(−8)
12.5	420 702.332(−6)	420 602.982(39)	420 589.935(24)[e]	420 589.935(24)[e]	420 596.098(198)[d]	420 608.897(49)
13.5	420 406.884(121)[d]	420 404.978(−53)	420 387.394(106)[d]	420 860.495(62)[d]	420 324.768(63)[d]	420 273.648(20)
14.5	420 118.407(−67)	420 121.048(98)[d]	420 119.814(−23)		420 105.848(39)	420 092.258(−1)
15.5	420 192.243(−2)	420 199.776(−74)	420 202.873(38)	420 201.167(41)	420 194.665(27)	420 183.307(35)
$N=14$						
11.5	450 914.830(−50)			450 881.854(7)		
12.5		450 966.374(−34)	450 954.306(−18)	450 945.700(16)		
13.5	450 674.380(29)	450 572.964(−53)	450 564.443(−509)[d]	450 567.039(18)	450 574.443(−29)	450 588.425(−8)
14.5	450 423.515(0)	450 418.604(−65)[d]	450 400.944(29)	450 375.571(10)	450 342.137(53)	450 292.653(3)
15.5	450 146.134(−92)[d]	450 148.343(22)	450 147.233(−38)	450 142.848(−9)	450 134.800(−18)	450 122.816(−39)
16.5			450 209.800(−45)	450 212.468(2)	450 210.951(28)	450 195.035(10)

[a]Standard deviation of the fit is 25.4 MHz. Calculated frequencies were obtained from the molecular constants given in Table II.
[b]Quantum numbers of the lower level for the transition, $(J+1,N+1,F+1)\leftarrow(J,N,F)$.
[c]Numbers in parentheses represent $\nu_{\text{obs.}}-\nu_{\text{calc.}}$ (kHz) from the least-squares fit. Subscripts denote quantum number, F.
[d]Not included in the least-squares fit.
[e]Unresolved lines.

TABLE II. Molecular constants of MnO ($X\ ^6\Sigma^+$) (MHz).[a]

	Present study	IMF[b]	Optical[c]	ESR[d]
B	15 025.814 87(41)	15 025.9	15 026.11(135)	
D	0.021 554 85(128)		0.021 67(39)	
λ	17 198.00(36)	17 200	16 900	
λ_D	−0.069 646(110)			
Θ	−14.67(31)			
γ	−70.7886(101)	−72	−56.4	
γ_D	−0.001 058 0(195)			
γ_S	0.009 79(82)			
b_F	479.861(100)	495		448(4)
b_{FD}	−0.001 450(74)			
b_S	−0.0382(153)			
c	−48.199(178)	−51		45(15)
eQq	−25.65(182)			
C_I	0.0631(49)			

[a]Values in parentheses are three standard deviations in units of the last significant digits.
[b]Intermodulated fluorescence, Ref. 8, in which experimental errors were not given.
[c]Reference 7.
[d]Reference 6.

for the third-order spin–orbit distortion term of the spin–rotation interaction,[16,18] and

$$H_{\rm iso}^{(3)}(K=3)=\sum_{i>j} T^1(\mathbf{I})T^1\{T^3[T^1(\mathbf{S}),T^2(\mathbf{s}_i,\mathbf{s}_j)],C^2\}/r_{ij}^3,$$

where i and j are electrons, r_{ij} is their separations, and

$$b_s=3\sum_{i>j}\langle\Lambda|C_0^2(\theta,\phi)/r_{ij}^3|\Lambda\rangle/(10\sqrt{14}),$$

for the third-order spin–orbit distortion of the Fermi contact interaction.[19] The matrix elements of the Hamiltonian are given in the literature[7,16–19] for Hund's case $(b)_{\beta J}$ basis function and the following coupling scheme of the angular momenta concerned: $J=N+S$ and $F=J+I(\mathrm{Mn})$. A least-squares fitting program was written for the analysis of the observed spectral lines. The energy levels were calculated by direct diagonalization of the Hamiltonian matrices.

An initial assignment of the observed lines was simply based on the predicted spectral pattern from the known molecular constants,[8] except for the higher-order terms. A trial least-squares fit suggested that the higher-order terms such as Θ, γ_s, C_I, and b_S were essential to obtain a small residual of the fit between observed and calculated frequencies. Furthermore, a centrifugal distortion effect for the Fermi contact term was necessary to attain a residual comparable to microwave spectroscopic measurement error. In the final fit several overlapping lines were fitted to calculated frequencies obtained by averaging the frequencies of component lines weighted by their relative intensity.[20] The standard deviation of the fit was 25.6 kHz, which is of the same order of magnitude as the frequency measurement errors. The determined molecular constants are listed in Table II.

DISCUSSION

This study is another demonstration that metal bearing molecules like MnO are efficiently generated in the gas phase by dc sputtering of the metal and/or metal containing compounds.[13,21–26] In contrast, it is difficult to generate the required concentrations for mm-wave spectroscopy using the more traditional method using a high-temperature flowing reactor. Furthermore, the molecules are produced at relatively low temperatures, greatly enhancing the pure rotational transition probability.

The molecular constants of MnO determined in the present study are compared in Table II with those reported in previous studies.[4–8] The rotational, centrifugal distortion, spin–spin coupling, spin–rotation coupling, and the two main hyperfine coupling constants agree well with those obtained by intermodulated fluorescence spectroscopy.[8] Eight minor molecular constants: three hyperfine [C_I(Mn), b_S(Mn), and eQq(Mn)]; two higher-order fine structure (γ_S and Θ); and three centrifugal distortion (λ_D, γ_D, and b_{FD}) were determined.

Hyperfine coupling constants

The ground electronic state of MnO is approximated by the following single configuration:[9]

$$X\ ^6\Sigma^+:(\mathrm{core})(9\sigma)^1(4\pi)^2(1\delta)^2,$$

where

$$(\mathrm{core})=(1\sigma)^2\sim(8\sigma)^2(1\pi)^4\sim(3\pi)^4.$$

The bonding orbital 8σ is strongly polarized toward the oxygen nucleus and the MnO bond is described mainly by a $\mathrm{Mn}^+(3d^5 4s^1)\mathrm{O}^-(2p^5)$ ionic structure. The above electronic configuration was used to interpret the hyperfine structure of MnO.

Since the Fermi contact coupling constant b_F reflects the s character of orbitals occupied by unpaired electrons, only the 9σ orbital must be considered in the interpretation of b_F. The 9σ orbital is given by a combination between the $3d\sigma$ and $4s$ orbitals of the Mn atom,

$$|9\sigma\rangle=c_1|4s(\mathrm{Mn}^+)\rangle-c_2|3d\sigma(\mathrm{Mn}^+)\rangle.$$

When the observed Fermi contact term is compared with that of the manganese cation, then $b_F=c_1^2 b_F(\mathrm{Mn}^+)/n$, where n is the number of unpaired electrons. Therefore, 4188 MHz for $b_F(\mathrm{Mn}^+)$[6] led c_1^2 to be 0.573: that is, the s character of the 9σ orbital is 57.3%. This means that $3d\sigma$ and $4s$ hybridization is nearly a perfect one to one mixture.

As Ferrante *et al.*[5] discussed the dipolar hfs constant c of MnO is related to a sum of contributions from the $3d$ unpaired electrons in the 9σ, 4π, and 1δ orbitals:

$$c=\frac{3}{2}g_s g_I\mu_s\mu_I\left[\frac{c_2^2}{5}\left\langle\frac{3\cos^2\theta-1}{r^3}\right\rangle_{3d\sigma}+\frac{2}{5}\left\langle\frac{3\cos^2\theta-1}{r^3}\right\rangle_{3d\pi}+\frac{2}{5}\left\langle\frac{3\cos^2\theta-1}{r^3}\right\rangle_{3d\delta}\right].$$

Using $c_2^2=0.427$, the angular expectation values for the $3d$ orbital, $\langle 3\cos^2\theta-1\rangle=4/7$ for $3d\sigma$, 2/7 for $3d\pi$, and $-4/7$ for $3d\delta$, and the radial expectation value for $3d$, $\langle 1/r^3\rangle_{3d}=4.167$ a.u.$^{-3}$,[27] c is calculated to be -54.0 MHz, which may be compared with the observed value of -48.168 MHz. When the approximation used in the calculation is taken into account, the agreement between the observed and calculated values is very good.

The electric quadrupole coupling constant of MnO comes from contributions due to the unpaired $3d\pi$ and $3d\delta$ electrons, the bonding electrons, and the polarization of the core electrons. Using the quadrupole moment of the manganese nucleus of 0.33×10^{-24} cm^2,[28] and the angular and radial expectation values given above, the eQq coupling constant due to the unpaired electrons is calculated to be 105.8 MHz. Since MnO has a relatively large dipole moment 3.22 D[11] like TiO(2.96 D),[29] the difference between the observed value of -25.65 MHz and the calculated unpaired electron contribution is assumed to be a contribution dominantly from the polarization of the core electrons. This corresponds well with that of TiO.[29]

Spin–rotation and nuclear spin–rotation coupling constants

The spin–rotation interaction should be dominated by the second-order contributions as given by[30,31]

$$\gamma^{(2)}=4\sum_n \frac{k_n\langle X\ ^6\Sigma^+|BL_-|n,^6\Pi\rangle\langle n,^6\Pi|H_{\rm el}^{\rm SO}|X\ ^6\Sigma^+\rangle}{E_\Pi-E_\Sigma},$$

where L_- is the ladder operator of the electronic angular momentum, $H_{\rm el}^{\rm SO}$ is the spin–orbit interaction, and k_n is either $+1$ or -1 according to whether the $n\ ^6\Pi-X\ ^6\Sigma^+$ excitation arises from an unoccupied or an occupied orbital.[32] Since the observed spin–rotation coupling constant is negative, the dominant perturbing excited state should be the $^6\Pi_i$ state under the assumption of the single perturber. Pinchemel and Schamps[9] reported the *ab initio* calculated excitation energies for all the low-lying configurations of MnO. Only regular $^6\Pi$ states and no inverted $^6\Pi$ states were predicted. Possible candidates of the perturber of the $X\ ^6\Sigma^+$ state may have the following configurations:

$$^6\Pi_i:(\text{core})(8\sigma)^1(3\pi)^4(9\sigma)^1(4\pi)^3(1\delta)^2$$

and

$$^6\Pi_i:(\text{core})(8\sigma)^2(3\pi)^3(9\sigma)^2(4\pi)^2(1\delta)^2.$$

These possible perturbing states satisfy the sign of the observed γ, but do not explain its magnitude sufficiently when the excitation energies[11] of 8σ to 4π and 3π to 9σ and the $3d$ orbital components[9] of 8σ and 3π are used to estimate their second-order contributions. This implies that the $3d$ character in the 8σ and/or 3π orbitals are larger than those given by the simple *ab initio* calculations.[9]

Similarly, the second-order contribution to the Mn nuclear spin–rotation coupling constant $C_I(\text{Mn})$ is related to $a|\gamma^{(2)}/\zeta(\text{Mn}^+)|$,[33] where a is the nuclear spin–orbit coupling constant and $\zeta(\text{Mn}^+)$ is the spin–orbit constant of the Mn atomic ion. If a of 549.8 MHz, calculated from $\langle r^{-3}\rangle_{3d}$,[27] $\zeta(\text{Mn}^+)$ of 392 cm^{-1},[31] and the observed values of γ are used in this relation, C_I is calculated to be 0.003 MHz, which is far from the observed value of 0.063 MHz. These results obtained for the spin–rotation and nuclear spin–rotation coupling constants suggest that a simple and single perturber treatment is not applicable to the interpretation of the two coupling constants.

Spin–spin coupling constant

The major contribution to the spin–spin coupling constant of the ground state is indirect second-order spin–orbit interaction with nearby electronic states. Since the selection rule for the spin–orbit interaction is given by $\Delta S=0,\ \pm1$, and $\Sigma^\pm-\Sigma^\mp$, the main perturber within the configuration of $(9\sigma)^1(4\pi)^2(1\delta)^2$ may be the $^4\Sigma^-$ state among nine available Σ states.[31] Hence,

$$\lambda^{(2)}=\frac{1}{8}\frac{|\langle^4\Sigma^-|H_{\rm el}^{\rm SO}|X\ ^6\Sigma^+\rangle|^2}{E(^4\Sigma^-)-E(X\ ^6\Sigma^+)}\approx\frac{\zeta(\text{Mn}^+)^2}{8\,\Delta E}.$$

The observed spin–spin coupling constant results in an excitation energy of 33 500 cm^{-1} for the $^4\Sigma^-$ state. There have been no observations or predictions of such a state.

Higher-order spin–orbit distortion terms

The third- and fourth-order spin–orbit distortion terms Θ, γ_s, and b_s are given sums over products of spin–orbit matrix elements, and are not easy to interpret, especially when the detailed electronic structure of MnO is not available. However, it is worthwhile assessing the magnitudes of these higher-order terms so as to carry out the analysis of microwave spectroscopic lines within their measurement errors.

The fourth-order spin–spin coupling term $|\Theta|$ is approximated to $\zeta(\text{Mn}^+)^4/\Delta E^3$,[16,17] where ΔE is the energy separation between the closest perturbing excited state and the ground state. The energy separation of 33 500 cm^{-1} derived above and the spin–orbit coupling constant for Mn^+ gives $|\Theta|$ of 18.8 MHz, which corresponds well to the observed value of -14.67 MHz.

Similarly, the third–order spin–rotation coupling constant γ_s is predicted to have a magnitude given by $\zeta(\text{Mn}^+)^2\Delta B/(\Delta E)^2$,[16] where ΔB is the difference between the rotational constants of the two states concerned. Thus, ΔB is calculated to be 71 MHz, which may be acceptable as a shift of the rotational constant from the ground state to the excited state.

Finally the third-order spin–orbit distortion to the Fermi contact term $|b_s|$ is predicted to have a magnitude given by $\zeta(\text{Mn}^+)^2|b_{\rm F}|/(\Delta E)^2$.[19] If the observed value of $b_{\rm F}$, 479.861 MHz, is used in this relation, $|b_s|$ is calculated to be 0.066 MHz, which compares with the observed value of -0.0379 MHz.

In conclusion, in the present paper we report the first microwave spectroscopic detection of the MnO radical in the $^6\Sigma^+$ ground electronic state by using a novel method for producing a refractory metal bearing transient species in a

microwave absorption cell of large volume. The detailed and precise determination of the molecular constants including higher-order spin–orbit distortion constants, which are characteristic of high-spin radicals, are given and are used to probe the molecular orbitals of MnO.

ACKNOWLEDGMENT

The authors thank Timothy C. Steimle for his critical reading of the manuscript and helpful discussions.

[1] A. J. Merer, Annu. Rev. Phys. Chem. **40**, 407 (1989).
[2] C. W. Bauschlicher, Jr. and P. Maitre, Theor. Chim. Acta **90**, 189 (1995).
[3] S. Gupta, Z. Phys. **91**, 471 (1934).
[4] B. Pinchemel and J. Schamps, Can. J. Phys. **53**, 431 (1975).
[5] R. F. Ferrante, J. L. Wilkerson, W. R. M. Graham, and W. Weltner, Jr., J. Chem. Phys. **67**, 5904 (1977).
[6] C. A. Baumann, R. J. Van Zee, and W. Weltner, Jr., J. Phys. Chem. **86**, 5084 (1982).
[7] R. M. Gordon and A. J. Merer, Can. J. Phys. **58**, 642 (1980).
[8] A. G. Adam, Y. Azuma, H. Li, A. J. Merer, and T. Chandrakumar, Chem. Phys. **152**, 391 (1991).
[9] B. Pinchemel and J. Schamps, Chem. Phys. **18**, 481 (1976).
[10] M. Dolg, U. Wedig, H. Stoll, and H. Preuss, J. Chem. Phys. **86**, 2123 (1987).
[11] E. G. Bakalbassis, M-A. D. Stiakaki, A. C. Tsipis, and C. A. Tsipis, Chem. Phys. **205**, 389 (1996).
[12] S. Saito and M. Goto, Astrophys. J. **410**, L53 (1993).
[13] K. Namiki and S. Saito, Chem. Phys. Lett. **252**, 343 (1996).
[14] C. H. Townes and A. L. Schawlow, *Microwave Spectroscopy* (McGraw-Hill, New York, 1955), Chap. 11.
[15] R. A. Frosch and H. M. Foley, Phys. Rev. **88**, 1337 (1952).
[16] J. M. Brown and D. J. Milton, Mol. Phys. **31**, 409 (1976).
[17] S. M. Corkery, J. M. Brown, S. P. Beaton, and K. M. Evenson, J. Mol. Spectrosc. **149**, 257 (1991).
[18] T. Nelis, J. M. Brown, and K. M. Evenson, J. Chem. Phys. **92**, 4067 (1990).
[19] A. S-C. Cheung and A. J. Merer, Mol. Phys. **46**, 111 (1982).
[20] A. R. Edmonds, *Angular Momentum in Quantum Mechanics* (Princeton University Press, Princeton, NJ, 1957).
[21] S. Takano, S. Yamamoto, and S. Saito, (to be published).
[22] M. Goto, S. Takano, S. Yamamoto, H. Ito, and S. Saito, Chem. Phys. Lett. **227**, 287 (1994).
[23] T. Oike, T. Okabayashi, and M. Tanimoto, Astrophys. J. **445**, L67 (1995).
[24] M. Tanimoto, S. Saito, and T. Okabayashi, Chem. Phys. Lett. **242**, 153 (1995).
[25] T. Okabayashi and M. Tanimoto, J. Chem. Phys. **105**, 7421 (1996).
[26] T. C. Steimle, K. Namiki, and S. Saito, J. Chem. Phys. (in press).
[27] S. Fraga, J. Karwowski, and K. M. Saxena, *Handbook of Atomic Data* (Elsevier, Amsterdam, 1976).
[28] J. Dembczy'nski, W. Ertmer, U. Johann, S. Penselin, and P. Stinner, Z. Phys. A **291**, 207 (1979).
[29] D. A. Fletcher, C. T. Scurlock, K. Y. Jung, and T. C. Steimle, J. Chem. Phys. **99**, 4288 (1993); also, T. C. Steimle and J. E. Shirley, *ibid.* **91**, 8000 (1989).
[30] J. M. Brown, E. A. Colbourn, J. K. G. Watson, and F. D. Wayne, J. Mol. Spectrosc. **74**, 294 (1979).
[31] H. Lefebvre-Brion and R. W. Field, *Perturbations in the Spectra of Diatomic Molecules* (Academic, Orlando, 1986).
[32] R. F. Curl, Jr., J. Chem. Phys. **37**, 779 (1962).
[33] Y. Endo, S. Saito, and E. Hirota, J. Mol. Spectrosc. **97**, 204 (1983).